

BEAM OPTICAL SIMULATION IN A PROPOSED MAGNETIC EINZEL LENS

M. H. Rashid[#] and A. Chakrabarty, VECC, 1/AF- Bidhannagar (Salt Lake), Kolkata- 700064, India

Abstract

Magnetic scalar potential and field distributions along the central axis of a magnetic einzel lens consisting of a pair of axisymmetric iron yoked anti-solenoids have been evaluated using a simple closed form of analytical expressions. The magnetic field distribution is used to track single charged particles as well as ion beam through lens segmentation method. The method facilitates in evaluation of optical properties as well as aberration coefficients of the lens. Application of such doublet solenoid lens in transporting low energy ion beam introduces nominal rotation of the beam as well as least entangling between transverse phase spaces of the beam. So, instead of single solenoid, it is always beneficial to use a magnetic einzel lens in beam optical systems.

INTRODUCTION

The early application of the lens is traced back with the advent of electron microscope, which need very powerful, flexible lens with least aberrations. The lenses are used widely in beam handling devices like ion-implanters, spectrometers, charge and mass analyzers and beam transport lines associated with particle accelerators.

An einzel lens, at the first instance, indicates an electrostatic rotationally symmetric uni-potential lens consisting of three coaxial electrodes. The electric field has exact mirror symmetry about the centre and charged particles passing through the lens are unaffected energy-wise and focused down-stream in transverse direction.

A magnetic einzel lens (MEL) [1, 2] is envisaged in the similar way using two equally and oppositely charged solenoids such that the magnetic field has exact mirror symmetry about the centre in between the solenoids and charged particles with some rigidity passing through the lens are theoretically unaffected rotation-wise. The total magnetic scalar potential on the axis is just superposition of the potentials at the circular openings of the solenoids and given by a closed form of analytical expressions. The magnetic field and its derivative are obtained as analytical expressions. The field configuration depends on the solenoid geometrical parameters and its excitation. The advantage of a MEL over electrostatic one should be mentioned that no electric insulation is needed and voltage breakdown does not happen. But it consumes and dissipates electric power and there is an essential need for cooling. Operation and removal of astigmatism is straight forward as the beam emerges finally without beam rotation in such lens. Magnetic materials with high magnetic permeability are used in such lens to reduce magneto-motive force (electric power) and shield the stray magnetic field.

[#]E-mail: haroon@vecc.gov.in

Details of aberration coefficients have been discussed in [2, 3, 4]. The aberrations rotate and blur the image shape with increased size. Lens aberrations can be reduced by decreasing the convergence angle of the system, so that charged particles are confined close to the axis of the lens. The ratio of the solenoid length and diameter affects both aberration and magnification, so the geometrical dimension should be optimized while designing a MEL.

MAGNETIC EINZEL LENS

For a pair of coaxial wire loops with the origin of the z-axis at the centre of the gap between the loops, the potential and field respectively are given by Eqs. 1 and 2. They are obtained by superposition of potentials created by the two loops passing some electric current, 'NI'. The potential and field along the axis depends on the geometrical parameters (pole gap '2s' and diameter '2R') of the lens by the current loops (solenoid).

$$\phi_1(z) = \frac{(NI)R}{\pi s} (z_+ \tan^{-1} z_+ - z_- \tan^{-1} z_-) \quad (1)$$

$$B_z(z) = \frac{-\mu_0 NI}{2\pi s} \left(\frac{z_+}{1+z_+^2} + \tan^{-1} z_+ - \frac{z_-}{1+z_-^2} - \tan^{-1} z_- \right) \quad (2)$$

Where $z_{\pm} = (z \pm s)/R$.

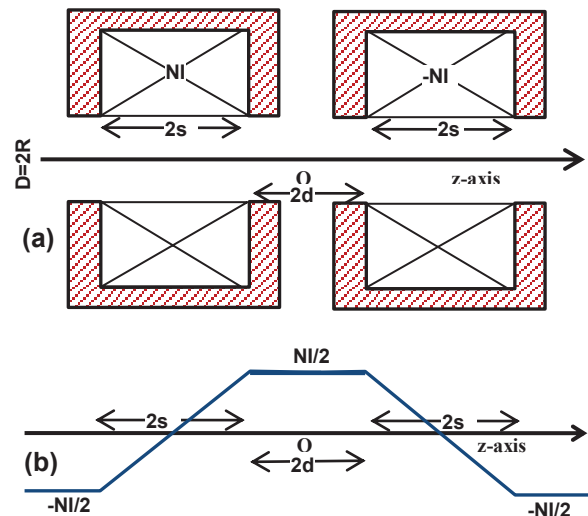


Figure 1: (a) Sketch of the MEL consisting of two solenoids, (b) Plot of scalar potential on the axis due to magneto-motive force NI.

Magnetic Potential and Field

We extend the single solenoid lens to two coaxial similar solenoids to form a MEL of diameter '2R' as shown in Fig. 1. The spacing between the two solenoids is 2d and the centres of the individual solenoids are situated

on either side of the origin are $t = \pm (s+d)$ distance. The superposed scalar potential and field respectively are expressed by Eqs. 3 and 4. When solenoids are placed side-by-side in same yoke, the potential and field due to a three aperture MEL are obtained by putting $d=0$.

$$\phi_2(z) = \phi_1\{z+(s+d)\} - \phi_1\{z-(s+d)\} \quad (3)$$

$$B_2(z) = B_1\{z+(s+d)\} - B_1\{z-(s+d)\} \quad (4)$$

Magnetic Field Evaluation

The plot of magnetic fields along the central axis of the MEL for different distance $2t=30, 20$ and 10 cm between the centre of the solenoids as well as for various NI can be evaluated analytically using Eqs. 3 and 4 respectively. The magnetic field distribution due to two solenoid lens (Fig. 2(a)) is evaluated using the 2D POISSON code [5] using the same geometrical structure and charging magneto-motive force, NI=37 kA, in the solenoids for $t = 10$ cm. The analytical (A) and numerical (N) fields are plotted along the central axis in Fig. 2(b) and found an excellent agreement within $\pm \leq 3.2\%$ between them. So, the analytical expression can be used straight way to assess the optical properties of the lens approximately.

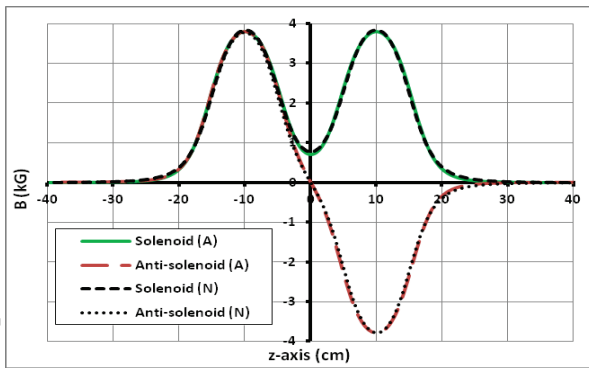
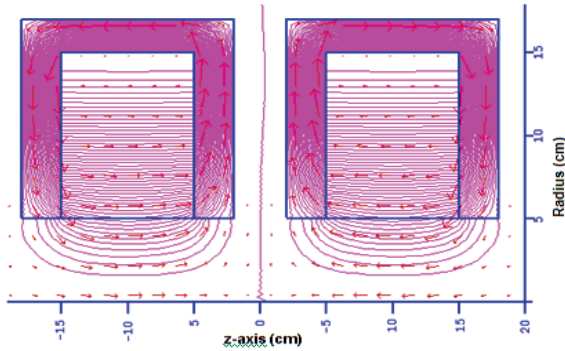


Figure 2: (a) Plot of computed magnetic lines of force, (b) Plot of axial field in solenoid and anti-solenoid case.

TRACKING OF CHARGED PARTICLE

Beam optical feature of a magnetic einzel lens has been discussed in [1] and now we will further investigate the beam rotation and the aberrations though charged particle tracking. We discussed the method of evaluating the optical properties by lens segmentation method there. It gives result with a little error.

Segmentation or Slicing Method

A method to construct a simple algorithm for low energy dynamics will require a large number of sufficiently small step polygons such that the field profiles change little and they are assumed to be almost constant in the step. The accuracy of the solution can be improved by increasing the number of segments (slice steps). This method was introduced and applied by Gans and subsequently by Timm [4, 6]. All segments may be of equal width as the j^{th} segment has $\delta z_j = h_j$ (adopted here) or of different width depending on the potential slope. Combination of segment method and matrix technique calculates beam optical properties when the axial potential and field distribution is known. The ray height from the central axis remains almost constant in a particular segment and the azimuth change in the adjacent slice is a little. The individual thin lens has power $1/F_j = k_j^2 h_j$, where $k_j = B_j / (2B\rho)$. The transport matrix for ‘n’ segments is given as product of the matrices of individual lenses (Eqs. 5).

$$M = \prod_{j=1}^n \begin{bmatrix} 1 - (h_j k_j)^2 / 2 & h_j (1 - (h_j k_j)^2 / 4) \\ -h_j k_j^2 & 1 - (h_j k_j)^2 / 2 \end{bmatrix} \quad (5)$$

The optical features were also studied in [1] to evaluate the approximate focal length, $1/M(1,2)$ or using Eq. 6, principal plane and the beam envelop of a beam of certain phase space area by adopting the above discussed method.

$$\frac{1}{F} = \sum_{j=1}^N \frac{1}{F_j} = \sum_{j=1}^N k_j^2 h_j \quad (6)$$

Evaluation Lens Aberrations

The spherical (C_s) and chromatic (C_c) aberration coefficients have been given considerable attention in the present research, since they are the two most important aberrations in beam optical system of charged particles. As charging power (NI) increases, C_s does not increase so rapidly as C_c . F_1 is the lens focal length at image side. It is convenient to express starting parameters of particle tracking as in Eq. 7 for aberration evaluation and two rays are distinguished by subscripts ‘g’ and ‘h’. They start far-off and on the z-axis with slope 0 and 45 deg. respectively.

$$r_g(z_0) = r_h'(z_0) = 1 \text{ and } r_g'(z_0) = r_h(z_0) = 0 \quad (7)$$

Spherical aberration is the 3rd order geometrical aberration that arises from the terms in r^3 in expansion of magnetic field, which is ignored in the paraxial approximation. This aberration starts from a point object on the beam optics. Non-paraxial rays passing through the outer zones of the lens are refracted more strongly and cross the axis before the crossing point on the paraxial rays. The aberration Fig. 3 is a circle of radius $r_{sa} \propto C_s \alpha^3$ where C_s represents the 3rd order spherical aberration coefficient and the maximum angle, $\frac{1}{2}\alpha$. But the smallest size of the beam does not occur at the image-plane but at a distance $C_s \alpha^2$ in front of the image-plane.

$$C_s = \frac{1}{12} \int_{z_0}^{z_f} (16k(z)^4 + 5k(z)^2 - k(z)k(z)''') r_h^4 dz \quad (8)$$

$$C_{sp} = \frac{1}{4} \int_{z_0}^{z_f} k(z) \{3k(z)^2 + r_g' / r_g\} r_g^2 dz \quad (9)$$

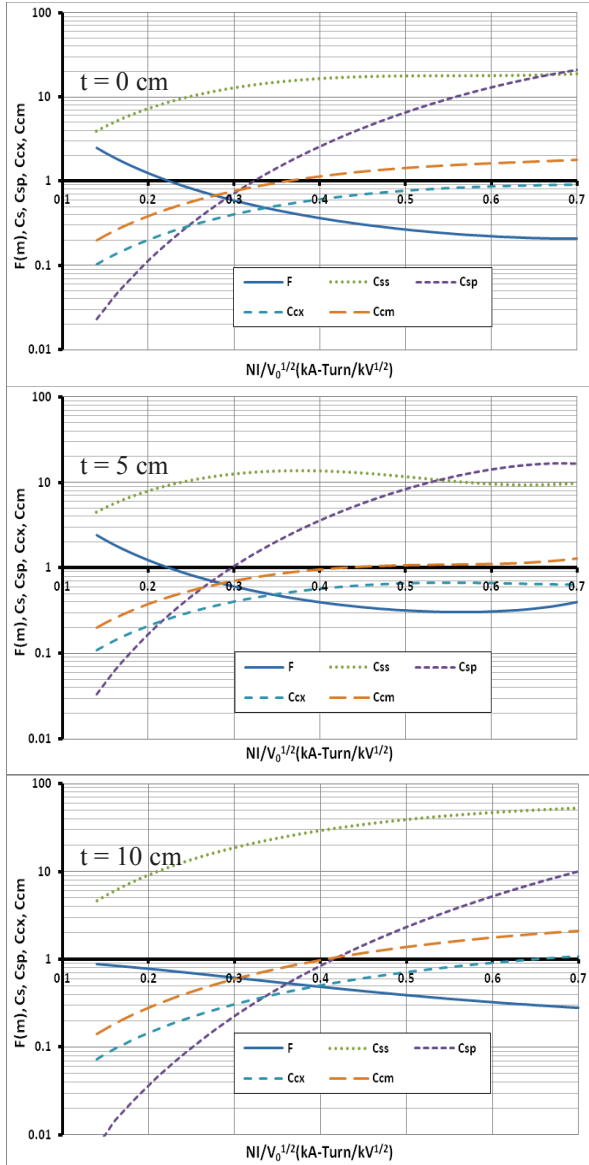


Figure 3: Focal length and various aberration coefficients for $t=0, 5, 10$ cm.

At higher excitation the value of aberrations are high. In the rotation free mode useful reduction of dispersion due to spiral aberration (Eq. 9) is possible. It is easy in two lens system to correct the rotation coefficient, dispersion but it is difficult to correct at the same time the off axis aberrations of chromatic change due to magnification and rotation.

The change in radius $r_{ca} \propto C_c \alpha (\delta E/E)$ of the image is introduced due to the chromatic aberration and energy spread, δE of the injected beam. It is called the disc of smallest confusion and has a radius $r_{sa}/4$. The chromatic aberration due to a cylindrical lens like solenoid due to axial beam path, beam magnification and beam rotation are given respectively by Eqs. 10, 11 & 12.

$$C_{cx} = \int_{z_0}^{z_f} k(z)^2 r_h^2 dz \quad (10)$$

$$C_{cm} = \int_{z_0}^{z_f} k(z)^2 r_h r_g dz \quad (11)$$

$$C_r = \frac{1}{2} \int_{z_0}^{z_f} k(z) dz \quad (12)$$

We track the r_g and r_h trajectories throughout the lens using the initial values stipulated by Eq. 7. The track coordinates and slopes of the trajectories are used to integrate the aberration equations incorporating the variable strength of the thin lenses along the z -axis starting from z_0 to z_f . The focal length as well as the aberrations coefficients changes with $NI/(V_0)^{1/2}$ for NI in kA-turn and initial accelerating voltage, $V_0=10000$ V (constant here). The beam rigidity of the particle is taken to be 0.04 T-m. The aberration coefficient due to rotation of the beam is maximum and almost zero respectively in a similarly and oppositely charged solenoid doublet. The oppositely charged doublet corresponds to the magnetic einzel lens. It is found that the ratio C_s/F remains almost constant and C_c/F increases almost linearly with excitation.

CONCLUSIONS

The theory proposed in this paper for the magnetic einzel lens consisting of two anti-solenoids also promises to give accurate optical properties and thus the method turns into a tool to design lens consisting of magnetic solenoids for various applications. Study of a rotationally symmetric combined electrostatic and magnetic einzel lens by this method will prove to be vital for its probably accurate design and proper applications in various beam optical devices including rotation free beam transport.

REFERENCES

- [1] M.H. Rashid and C. Mallik, Proc. CYCLOTRONS-2010, Lanzhou, China **MOPCP044** (2010).
- [2] N. Baba et al., J. Phys. E: Instrum. **12** (1979) 525.
- [3] A.B. Elkareh and J.C.J Elkareh, "Electron Beam Lenses and Optics", Vol. 1, Academic Press, London, 19.
- [4] A. Septier, *Focusing of Charged Particles*, Vol II Academic Press Inc., New York, (1967) p. 315.
- [5] M. T. Menzel et al., POISSON/SUPERFISH Group Codes, LANL Report **LA-UR-87-115** (1987).
- [6] U. Timm, Z. Naturforsch. **10a** (1955) 593.